1521-0103/376/3/322–329$35.00
THE JOURNAL OF PHARMACOLOGY AND EXPERIMENTAL THERAPEUTICS

https://doi.org/10.1124/jpet.120.000158
J Pharmacol Exp Ther 376:322–329, March 2021

Calculation of an Apical Efflux Ratio from P-Glycoprotein (P-gp) In Vitro Transport Experiments Shows an Improved Correlation with In Vivo Cerebrospinal Fluid Measurements in Rats: Impact on P-gp Screening and Compound Optimization[S]

Holger Fischer, Claudia Senn, Mohammed Ullah, Carina Cantrill, Franz Schuler, and Li Yu

Roche Pharmaceutical Research and Early Development, DMPK/PD project leader (H.F.), Comparative Pharmacology (C.S.), Investigative Safety, Pharmaceutical Sciences (M.U., C.C.), and Immunology, Infectious Disease and Ophthalmology (F.S.), Roche Innovation Center, Basel, Switzerland; and Roche Pharmaceutical Research and Early Development, Pharmaceutical Sciences, Roche Translational and Clinical Research Center, Inc., and LIYU Pharmaceutical Consulting LCC, New Jersey, USA (L.Y.)

Received June 8, 2020; accepted December 2, 2020

ABSTRACT

P-glycoprotein (P-gp) is a major blood-brain barrier (BBB) efflux transporter. In vitro approaches, including bidirectional efflux ratio (ER), are used to measure P-gp–mediated transport, but findings can be inconsistent across models. We propose a novel, more physiologically relevant, in vitro model: unidirectional apical efflux ratio (AP-ER)—a ratio of permeability rates at the apical side of the BBB with and without P-gp inhibitor. To test our approach, ER and AP-ER were calculated for 3227 structurally diverse compounds in porcine kidney epithelial cells (LLC-PK1) overexpressing human or mouse P-gp and classified based on their passive transcellular P-gp permeability or charged properties. In vivo rat infusion studies were performed for selected compounds with high ER but low AP-ER. One-third of the 3227 compounds had bidirectional ER that was much higher than AP-ER; very few had AP-ER higher than ER. Compounds with a large difference between AP-ER and ER were typically basic compounds with low-to-medium passive permeability and high lipophilicity and/or amphiphilicity, leading to strong membrane binding. Outcomes in the human model were similar to those in mice, suggesting AP-ER/ER ratios may be conserved for at least two species. AP-ER predicted measured cerebrospinal fluid (CSF) concentration better than ER for the five compounds tested in our in vivo rat infusion studies. We report superior estimations of the CSF concentrations of the compounds when based on less resource-intensive AP-ER versus classic ER. Better understanding of the properties leading to high P-gp–mediated efflux in vivo could support more efficient brain-penetrant compound screening and optimization.

SIGNIFICANCE STATEMENT

To address inconsistencies associated with the historical, bidirectional efflux ratio (ER) calculation of P-glycoprotein–mediated transport, we propose to use the novel, more physiologically relevant, unidirectional apical efflux ratio (AP-ER) model. In vitro experiments suggested that compounds with strong membrane binding showed the largest difference between AP-ER and ER, and in vivo infusion studies showed that AP-ER predicted cerebrospinal fluid concentrations of compounds better than ER; outcomes in the human model were similar to those in mice.

Introduction

Since the discovery of the relevance of P-glycoprotein (P-gp) as an efflux transporter at the blood-brain barrier (BBB) (Schinkel et al., 1995), several other promiscuous efflux transporters, which transport compounds from the brain back into the plasma, have been identified (Giacomini et al., 2018). It is very interesting to note, however, that after almost 25 years of research in this area, P-gp remains among the most relevant of the transporters acting on the distribution of various xenobiotics at the BBB (De Lange et al., 2018).

Preclinical animal models, in particular rodents, are routinely used in drug discovery to study the impact of P-gp on BBB penetration. However, such studies require complex surgical techniques (i.e., for cerebrospinal fluid [CSF] sampling), and the collection of brain tissue means that large numbers of animals need to be sacrificed. Recently, positron emission tomography–based techniques have been proposed as a way to follow the kinetics of P-gp substrates in vivo in rodents, nonhuman primates, and humans (Bankstahl et al., 2008; Schou et al., 2015; Pottier et al., 2016; Tournier et al., 2019). Positron emission tomography imaging techniques are, however, very costly and are thus reserved for the assessment

This study was supported by F. Hoffmann-La Roche Ltd./Genentech Inc.
Primary laboratory of origin: Roche Pharmaceutical Research and Early Development, Roche Innovation Center (Basel, Switzerland).
https://doi.org/10.1124/jpet.120.000158.
[S] This article has supplemental material available at jpet.aspetjournals.org.

ABBREVIATIONS: A→B, apical to basolateral; AP-ER, apical efflux ratio; B→A, basolateral to apical; BBB, blood-brain barrier; CSF, cerebrospinal fluid; $C_{u,p}$, free plasma concentration; ER, efflux ratio; MRD, multidrug resistance protein; P_{app}, apparent permeability; P-gp, P-glycoprotein.

of target occupancy in nonhuman primates for advancing clinical candidate drugs. There is, therefore, a clear need for robust in vitro P-gp models that are predictive of the in vivo situation and can be applied at an early discovery stage. Although a multitude of vesicle- and cell-based systems are available to assess P-gp transport (Litman et al., 1997; Eytan et al., 1997; Landwojtowicz et al., 2002; Schwab et al., 2003; Brouwer et al., 2013), in vitro to in vivo translation remains a significant challenge (Hammarlund-Udenaes et al., 2008). Indeed, results from such different models often lack consistency and are not readily extrapolated (Saaby and Brodin, 2017).

The method most widely used in the pharmaceutical industry and that is recognized by the regulatory authorities to assess P-gp in vitro is the bidirectional transport model, which consists of polarized cell monolayer cultures expressing P-gp [e.g., the porcine kidney epithelial cell line (LLC-PK1), Madin-Darby canine kidney cell line, or the human epithelial colon adenocarcinoma cell line, Caco-2] cultured on permeable filters. Asymmetry in the apparent permeability (P_{app}) of a compound across these cell monolayers is used to define the presence of efflux transport of a compound. P_{app} reflects the rate by which a compound penetrates a defined surface area; hence, $P_{app}^{B\rightarrow A}$ is the P_{app} in the basolateral-to-apical (B→A) direction, whereas $P_{app}^{A\rightarrow B}$ is the P_{app} in the apical-to-basolateral (A→B) direction. The bidirectional efflux ratio (ER) of $P_{app}^{B\rightarrow A}$ over $P_{app}^{A\rightarrow B}$, which cancels out the contribution of passive permeability, yields a measure of P-gp transport activity for the compound of interest.

ER has been used in numerous publications to optimize compounds against P-gp–mediated efflux (Desai et al., 2013). Analysis of marketed drugs revealed that compounds targeting the central nervous system generally display ERs less than 3, thus providing a categorization of brain-penetrant compounds based on measured ER (Kikuchi et al., 2013; Poirier et al., 2014). Indeed, the ER parameter has been used to successfully establish a quantitative relationship between the free plasma concentration and the measured CSF concentration ratio in rodents and nonrodents for compounds with good passive permeability (Ohe et al., 2003; Tang et al., 2009; Caruso et al., 2013). Accordingly, during drug discovery screening, compounds with ER greater than 3 are usually considered unlikely to sufficiently reach the brain (i.e., they would be predicted to have low CSF exposures) and are therefore discarded. However, in this study, we will show that a number of compounds with very high ERs (>10) readily reach the CSF in rats in vivo at pharmacologically relevant concentrations. To address this discrepancy, we propose a new in vitro methodology, termed the apical efflux ratio (AP-ER), which identifies these brain-penetrant compounds and leads to improved correlation between measured CSF in vivo and free plasma concentration at steady state. Finally, we present results of compartmental modeling that helps to determine whether high ERs are due to low passive permeability of the compound or a high P-gp–mediated transport rate.

Material and Methods

Theoretical Section

A Three-Compartment Kinetic Model to Describe Transport Across Cell Monolayers. Transport across cell monolayers can be described by a three-compartment model, as shown schematically in Fig. 1. P-gp is located at the apical membrane of the cellular monolayer where it transports compounds back into the apical compartment (blood); a "vacuum cleaner" model has been proposed to describe this P-gp–mediated efflux of compounds at the BBB. In this model, the membrane-bound compound is recognized by P-gp and expelled back to the apical compartment (Higgins and Gottesman, 1992); various studies have since confirmed this hypothesis (Shapiro and Ling, 1997; Pleban et al., 2005).

All the equations described in this section are listed in Supplemental Table 1.

ER is calculated by dividing $P_{app}^{B\rightarrow A}$, obtained from dosing the compound into the basolateral compartment (interstitial side of the brain), by $P_{app}^{A\rightarrow B}$, where the same compound at the same concentration and pH is dosed into the apical compartment (e.g., for the BBB) (eq. 1):

$$ER = \frac{P_{app}^{B\rightarrow A}}{P_{app}^{A\rightarrow B}} \quad (1)$$

P_{app} rates can be obtained from the three-compartment model, as depicted in Fig. 1. $P_{app}^{A\rightarrow B}$ is described by a time-dependent change of compound concentration in the basolateral compartment B (dB/dt) with the compound being added to the apical side (eq. 2):

$$P_{app}^{A\rightarrow B} = \frac{V}{S \cdot C_0} \cdot \frac{dB}{dt} \quad (2)$$

where S refers to the surface area (square centimeters) available for permeability, C_0 defines the initial substrate concentration in the donor compartment, and V is the volume of the receiver compartment.

Similarly, $P_{app}^{B\rightarrow A}$ is described by a time-dependent change in the compound concentration in the apical compartment A (dA/dt) with the test compound being added to the basolateral side (eq. 3).

$$P_{app}^{B\rightarrow A} = \frac{V}{S \cdot C_0} \cdot \frac{dA}{dt} \quad (3)$$

The compound flux rates in and out of each compartment can be described by three differential equations (eqs. 4–6):

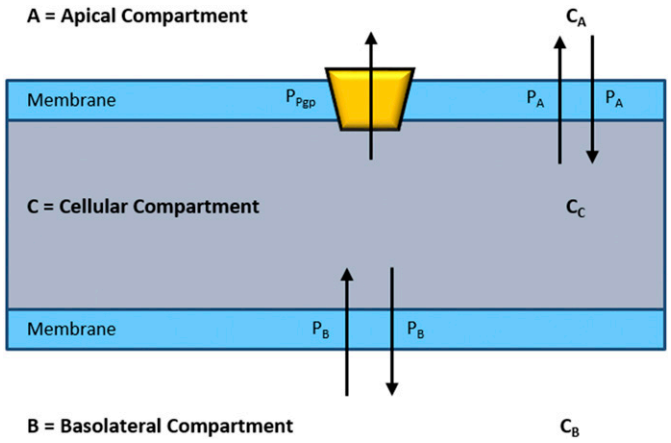

Fig. 1. Three-compartment model describing the diffusion process in polarized cell monolayers by passive diffusion (P_A, P_B) and active transport (P_{Pgp}). It is assumed that the passive permeability P_A and P_B in or out of the cellular compartment is identical in both directions. Although the binding sites of P-gp substrates (P_{Pgp}) are located within the membrane, it is assumed that P-gp mainly modifies the compound concentration in the cellular and apical compartments at "quasi" steady state conditions. $c_A/c_B/c_C$, substrate concentration in the apical/basolateral/cellular compartment; P_A/P_B, passive permeability at the apical/basolateral site; P_{Pgp}, permeability at the binding site assumed to be between the middle and outer leaflet of the apical membrane.

$$V\frac{dA}{dt} = \left(- P_A c_A + P_A c_C + P_{P\text{-}gp} c_C \right) S \quad (4)$$

$$V\frac{dC}{dt} = \left(P_A c_A - P_A c_C - P_{P\text{-}gp} c_C - P_B c_C + P_B c_B \right) S \quad (5)$$

$$V\frac{dB}{dt} = \left(- P_B c_B + P_B c_C \right) S \quad (6)$$

In these equations, dA/dt, dC/dt, and dB/dt represent the rate of change in the apical, cellular, and basolateral compartments, respectively. P_A and P_B represent the passive permeability at the apical and basolateral sites, respectively, and c_A, c_B, and c_C refer to substrate concentration in the apical, basolateral, and cellular compartments, respectively. $P_{P\text{-}gp}$ defines the permeability attributed to the active transport of a compound to the apical compartment at either of the three binding sites; two are assumed to be between the middle and outer leaflets of the apical membrane, and the third postulated binding site is close to the inner leaflet of the apical membrane (Wise, 2012). Although the P-gp binding sites are located within the cellular membrane, we assume that P-gp mainly affects the compound concentration in the apical and cellular compartments.

At "quasi" steady state conditions (dC/dt = 0), the concentration in the cellular compartment (c_c) can be derived from eq. 5 to give eq. 7:

$$c_c = \frac{P_A c_A + P_B c_B}{P_A + P_B + P_{P\text{-}gp}} \quad (7)$$

As a result, $P_{app}^{A \to B}$ is obtained by a combination of eqs. 2, 6, and 7 assuming that $c_0 \sim c_A$ and $c_B \sim 0$ under the initial conditions (eq. 8):

$$P_{app}^{A \to B} = \frac{P_A \cdot P_B}{P_A + P_B + P_{P\text{-}gp}} \quad (8)$$

Similarly, $P_{app}^{B \to A}$ is calculated by combining eqs. 3, 4, and 7, with $c_0 \sim c_B$ and $c_A \sim 0$ (eq. 9):

$$P_{app}^{B \to A} = \frac{\left(P_A + P_{P\text{-}gp} \right) \cdot P_B}{P_A + P_B + P_{P\text{-}gp}} \quad (9)$$

Combining eqs. 1, 8, and 9, the ER is defined by passive (P_A, P_B) and active ($P_{P\text{-}gp}$) transport permeability rates (eq. 10):

$$ER = \frac{P_A + P_{P\text{-}gp}}{P_A} \quad (10)$$

An alternative approach is to calculate the AP-ER, which depends on the permeability rates where the compound is applied from the apical compartment only with P-gp inhibitor ($P_{app}^{A \to B}(+I)$) and without P-gp inhibitor ($P_{app}^{A \to B}$) at the apical site (eq. 11):

$$AP^{-}ER = \frac{P_{app}^{A \to B}(+I)}{P_{app}^{A \to B}} \quad (11)$$

The apparent permeability with P-gp inhibitor can, therefore, be obtained from eq. 8 with $P_{P\text{-}gp} = 0$ (eq. 12):

$$P_{app}^{A \to B}(+I) = \frac{P_A \cdot P_B}{P_A + P_B} \quad (12)$$

A combination of eqs. 11, 12, and 8 defines AP-ER as a combination of permeability rates (eq. 13):

$$AP^{-}ER = \frac{P_A + P_B + P_{P\text{-}gp}}{P_A + P_B} \quad (13)$$

Subsequently, ER (eq. 10) and AP-ER (eq. 13) can be combined by substituting $P_{P\text{-}gp}$, which yields eq. 14:

$$ER = \left(\frac{P_A + P_B}{P_A} \right) \cdot AP^{-}ER - \left(\frac{P_B}{P_A} \right) \quad (14)$$

If we assume that the passive permeability is the same at the apical and the basolateral sides ($P_A = P_B$) in eq. 14, ER is defined as (eq. 15):

$$ER = 2AP^{-}ER - 1 \quad (15)$$

Similarly, if we assume $P_A = P_B = P$ in eq. 13, we can calculate $P_{P\text{-}gp}$ as (eq. 16):

$$P_{P\text{-}gp} = (AP^{-}ER - 1) \cdot 2P \quad (16)$$

Eq. 15 defines the conceptual relationship between the classic bidirectional ER and the new AP-ER. Eq. 16 separates the passive permeability contribution to AP-ER from the P-gp–mediated permeability.

Experimental Methods

In Vitro P-gp Measurements. Bidirectional permeability and P-gp efflux were measured using LLC-PK1, kindly provided by Dr. A. Schinkel (The Netherlands Cancer Institute, Amsterdam, The Netherlands). LLC-PK1 cells were selected because they offer the advantage of consistently overexpressing human P-gp (allowing for high sensitivity and reproducibility) in a host cell line that is not of human origin (i.e., does not express endogenous human efflux transporters) (Kuteykin-Teplyakov et al., 2010). Although we cannot rule out the potential influence of endogenous porcine transporters in LLC-PK1 cells (Miyamoto et al., 2019), it is reasonable to expect that this is less of a concern than in more classically used cell lines such as Caco-2, which are of human origin and are known to endogenously express multiple human transporters at significant levels, including multidrug resistance-associated protein 2 (MRP2) and breast cancer resistance protein(BCRP), in addition to P-gp. LLC-PK1 were stably transfected with human or murine P-gp [multidrug resistance protein (MDR) 1, ATP-binding cassette sub-family B member 1 (ABCB1)], as previously described (Poirier et al., 2014). The P_{app} values related to transcellular transport, ER, AP-ER, and mean bidirectional passive permeability were calculated for 3227 compounds with a large range of biochemical properties (Supplemental Materials).

Briefly, on day 4 after plating, cell monolayers were evaluated for drug permeability in the A→B and B→A directions using a liquid handling robotic system (Tecan, Maennedorf, Switzerland). Unless otherwise stated, test compounds were dosed at 1 μM. Samples were collected from triplicate wells of donor and receiver compartments after a 3.5-hour incubation in the presence or absence of a P-gp inhibitor (1 μM, zosuquidar). Drug concentrations were measured by high-performance liquid chromatography–tandem mass spectrometry; recovery values in the range 70%–120% were considered acceptable.

Compounds were categorized according to their passive transcellular permeability in the P-gp in vitro assay ($P_{app}^{A \to B}(+I)$). Compound permeability was considered to be low when $P_{app}^{A \to B}(+I) \leq 10$ nm/s, low-to-medium when 10 nm/s$< P_{app}^{A \to B}(+I) \leq 50$ nm/s, medium-to-high when 50 nm/s$< P_{app}^{A \to B}(+I) \leq 100$ nm/s and high when $P_{app}^{A \to B}(+I) > 100$ nm/s.

Calculation of Molecular Charges. To classify the compounds according to their charged properties, we calculated the pKa value for all compounds with the MoKa software (Milletti et al., 2007) regularly trained with in-house compounds. At pH 7.4, compounds that were >10% positively charged (basic pKa >6.45) were considered basic; compounds with a negative charge >10% were considered acidic (acidic pKa <8.35); compounds with an acidic pKa <8.35 and a basic pKa >6.45 were considered ampholytic; and other compounds were considered neutral. From the 3227 compounds in the data set, 21% were bases, 9% were acids, 5% were ampholytes, and 65% were neutral.

Animal Experiments. All animal studies were performed in accordance with the Guide for the Care and Use of Laboratory Animals as adopted and promulgated by the US National Institutes of Health. The experimental preclinical testing protocols were approved by the Institutional Animal Care and Use Committee of the Cantonal Veterinary Office Basel, Switzerland. The animal facility was accredited by the Association for Assessment and Accreditation of Laboratory Animal Care.

Plasma Protein Binding Experiments with Rat Plasma. Plasma protein binding was determined using equilibrium dialysis as described by Banker et al. (2003) and Zamek-Gliszczynski et al. (2011). Briefly, dialysis sides of a 96-well high-throughput dialysis block (HTDialysis, Gales Ferry, CT) were loaded with 0.15 ml of Søerensen phosphate buffer (pH 7.5). An equal volume of plasma spiked with the test compound was added to the sample side of each well, and the dialysis unit was sealed with a semipermeable adhesive cover and incubated at 37°C (5% CO_2) for 5 hours. At the end of dialysis, plasma and buffer samples were retrieved, and drug concentrations were quantified using liquid chromatography–tandem mass spectrometry.

In Vivo Infusion Study in Rats with CSF Collection. To investigate whether ER or AP-ER was more relevant for estimating in vivo CSF concentrations, in vivo infusion studies in rats were performed using five compounds: RO1, RO2, RO3, RO4, and RO5. For RO1–4, age- and weight-matched male Sprague Dawley rats (three rats per time point) received a single intravenous bolus dose [in hydroxypropyl-γ-cyclodextrine and 1-methyl-2-pyrrolidone (70:30)] followed by intravenous infusion of the drug dissolved in vehicle [hydroxypropyl-γ-cyclodextrine:1-methyl-2-pyrrolidone (80:20)]. The RO5 compound was dissolved in 10 mM lactic acid and 5% glucose at pH 5.0 for administration (four rats per time point). This ensured that steady state was reached before CSF samples were taken. Animals were sacrificed 4–8 hours after the start of the infusion, and CSF, plasma, and brain samples were collected. To investigate whether transporters other than P-gp contributed to the active efflux, the same rat infusion experiments were repeated with and without the presence of tariquidar, a selective P-gp inhibitor. Experiments with the RO5 compound were not conducted in the presence of tariquidar, as RO5 steady state takes a long time to reach and it was considered that tariquidar infusions would not be tolerated by the animals. A detailed description of experimental design and collection schedule for plasma, CSF, and brain samples can be found in the Supplemental Materials and Supplemental Table 2.

Data Analysis. For the statistical analyses, only group mean and S.D. values were calculated for all in vitro and in vivo studies. Linear regression calculations were carried out in STATISTICA 12.0 (2013; StatSoft, Inc., Tulsa, OK).

Results

Calculation of the AP-ER as Unidirectional Measure for P-gp Substrate Activity. The most conventional way to determine P-gp–mediated transport activity is by measuring bidirectional transport rates (ER; eq. 1). Alternatively, AP-ER is calculated by using P_{app} from only one direction (A→B) with and without P-gp inhibitor as described in eq. 11. A compartmental modeling approach was used to mechanistically compare the two approaches, as outlined in the theoretical section. If we assume that passive permeability at the apical and basolateral sites are approximately identical ($P_A \sim P_B \sim P$) in eq. 14, a very simple relationship between the ER and the AP-ER is obtained (eq. 15).

Figure 2 shows the correlation between ER and AP-ER values for all compounds with multidrug resistance protein (mdr1a) P-gp transport data in our in-house data base (3227 compounds). The black solid line in Fig. 2 depicts the theoretical relationship (eq. 15) between the ER and AP-ER models: 64% of all compounds were within a 2-fold error margin (i.e., had equivalent ER and AP-ER). Interestingly, very few compounds (2%) were located below the line (i.e., had an AP-ER higher than ER), and the remaining 34% of compounds were above the 2-fold error line (i.e., had ER much higher than AP-ER).

Molecular Properties of Compounds with High Bidirectional ER but Low AP-ER. Our experiments demonstrated that $P_{app}^{A\rightarrow B}(+I)$, which represents passive permeability, and molecular charge both influence correlation between ER and AP-ER. Figure 2A presents correlation between ER and AP-ER according to $P_{app}^{A\rightarrow B}(+I)$ values. Generally, there was a trend for increased ER versus AP-ER with decreasing passive permeability values. In particular, compounds with low, low-to-medium or medium-to-high permeability showed a clear trend toward a larger difference between ER and AP-ER compared with high-permeability compounds; these compounds represented 35% of the entities with ER values more than 2-fold larger than AP-ER values and only 19% of compounds within the 2-fold error margin. Similar observations were made when considering molecular charge (Fig. 2B). Compounds with a very large difference between ER and AP-ER (upper left in Fig. 2B) were often compounds bearing a positive charge (basic); whereas, on average, compounds with a smaller difference between ER and AP-ER were neutral. Among compounds above the 2-fold error margin, 28% were basic, 51% were neutral, 11% acidic, and 10% amphoteric, whereas for compounds within the 2-fold error margin 16% were basic, 74% were neutral, 7% were acidic, and 3% were amphoteric.

Assessment of the AP-ER with Published CSF Concentrations. To assess whether ER or AP-ER more accurately describes P-gp efflux properties in vivo, we used a previously published quantitative linear relationship for compounds with low to medium/high passive permeability (Caruso et al., 2013), which contains the in vivo-measured CSF concentration in rats with the free plasma concentration ($C_{u,p}$). The influence of the in vitro ER on the in vivo–determined $CSF/C_{u,p}$ is depicted in the following equation, with a and b being regression coefficients (eq. 17):

$$\frac{CSF}{C_{u,p}} = b + a \cdot \frac{1}{ER \text{ or } AP^{-}ER} \tag{17}$$

From the 34 compounds that were published (Caruso et al., 2013) and where the primary data required to calculate ER and AP-ER were available (Supplemental Table 3), we derived the statistical parameters presented in Table 1. Our results suggest that in rats AP-ER is slightly better suited to describing measured CSF concentration than ER, as demonstrated by the higher r^2 (0.71 vs. 0.76); in addition, the coefficient was close to 1 (a = 1.04), and b was very small (b = –0.03).

In Vivo $CSF/C_{u,p}$ Concentration Ratio of Compounds with High Bidirectional ER But Low AP-ER. Infusion studies for the five analyzed compounds are summarized in Table 2. Comparison between the compartmental models for ER and AP-ER suggests that ER values should be approximately two times higher than AP-ER values (eq. 15). However, Fig. 2 shows that for some compounds, ER can be much higher than twice the AP-ER values. Detailed results for one of these compounds, RO1, which had an ER of 23 and AP-ER of 4, are

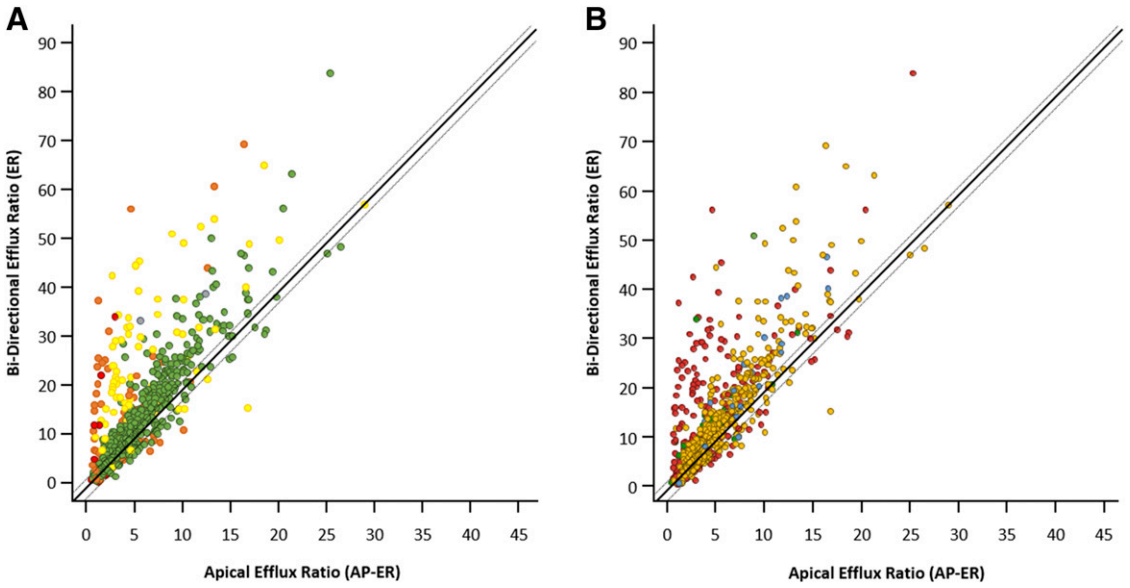

Fig. 2. ER vs. AP-ER calculated from the mouse mdr1a LLC-PK1 assay results. The black line represents results of the compartmental modeling (eq. 15) where ER = 2·AP-ER – 1. Dashed lines represent the 2-fold error lines accounting for experimental uncertainty. From the 3227 data obtained, 64% of all compounds fall within the 2-fold error margin, 34% are above the 2-fold error line, and only 2% are below the lower 2-fold error line. (A) Colors indicate four $P_{app}^{A\to B}(+I)$ permeability categories for passive permeability: $P_{app}^{A\to B}(+I)\leq 10$ nm/s, low (red); 10 nm/s$< P_{app}^{A\to B}(+I)\leq 50$ nm/s, low-to-medium (orange); 50 nm/s$<P_{app}^{A\to B}(+I)\leq 100$ nm/s, medium-to-high (yellow); $P_{app}^{A\to B}(+I)>100$ nm/s, high (green). (B) Color code indicates the following four groups according to their calculated pKa values: neutral (amber), basic (red), acidic (blue), and amphoteric (green). $P_{app}^{A\to B}(+I)$, apparent permeability from apical to basolateral site in the presence of an inhibitor.

described in Fig. 3. According to eq. 17, an approximately 6-fold higher CSF concentration is expected when calculated using AP-ER instead of ER. The measured CSF concentration revealed that using AP-ER in eq. 17 gives a much better estimation of the measured CSF concentration than using ER.

In the presence of tariquidar (i.e., based on AP-ER), the CSF concentration was equal to the free plasma concentration, which suggests that no other efflux or uptake system was involved in the disposition of RO1–4. In all rat infusion studies, calculated $CSF/C_{u,p}$ ratios using AP-ER were much closer to the measured $CSF/C_{u,p}$ ratios than calculated ratios using ER (Table 2).

Discussion

Conceptual Difference between the Unidirectional AP-ER and the Classic Bidirectional ER. Efflux values represent a method to assess the ability of compounds to be transported by ATP-binding cassette (ABC) transporters, including P-gp. Since the introduction of efflux values, experiments have been performed in a bidirectional transport assay where the contribution of active efflux by P-gp is assessed by dividing the apparent permeability from the basolateral side with the apparent permeability from the apical side (eq. 1; Fig. 4) to eliminate the contribution from passive permeability. Hence, ER is a descriptor that accounts only for the active efflux contribution. Consequently, the contribution of P-gp to ER is considered "twice" (reduced $P_{app}^{A\to B}$ and higher $P_{app}^{B\to A}$ due to P-gp contribution); therefore, ER is higher than AP-ER (for which only the reduced $P_{app}^{A\to B}$ is taken into account). This is reflected in the mathematical relationship between ER and AP-ER (eq. 15) where AP-ER is roughly half of the ER value. This difference is more pronounced for poorly permeable compounds, as they are more greatly affected by the active contribution of P-gp (eqs. 10 and 13). Although unidirectional measurements similar to AP-ER have been described previously (Thiel-Demby et al., 2004; Ohashi et al., 2019) and are able to differentiate strong and weak P-gp substrates, these studies also showed correlation between estimates based on unidirectional measurements and classic ER, and hence superiority of unidirectional measurements over bidirectional models was not described.

Despite the difference in absolute values, ~60% of the compounds in our in-house data base show a good correlation between ER and AP-ER. Furthermore, 38% of the compounds have ER values more than 2-fold higher than AP-ER values including some that have ER values more than 10-fold higher than AP-ER values. In contrast, very few compounds (2%) had an AP-ER higher than ER. Closer inspection of molecular properties revealed that compounds with a very high difference between AP-ER and ER are very often basic compounds with a lower passive permeability (Fig. 2) and a higher lipophilicity and/or high amphiphilicity leading to a stronger membrane binding and a lower than normal recovery from the assay (data not shown). In particular, the accumulation in lysosomes might have an effect on the permeability (Bednarczyk and Sanghvi, 2020) and thus also affect ER

TABLE 1

Summary of the linear regression analysis of eq. 17

$CSF/C_{u,p}$ values were taken from reference (Caruso et al., 2013). Only compounds from (Caruso et al., 2013) for which $P_{app}^{A\to B}$ (+I) and $P_{app}^{A\to B}$ were available to calculate AP-ER were selected. Primary data are available in the Supplemental Information.

Parameter	a (±S.E.)	b (±S.E.)	r^2	*n*
ER	0.89 ± 0.10	0.14 ± 0.05	0.71	34
AP-ER	1.04 ± 0.10	−0.03 ± 0.06	0.76	34

a and b are regression coefficients. P_{app} (+I), apparent permeability in the presence of an inhibitor.

TABLE 2

Comparison between the measured CSF/$C_{u,p}$ values of a rat infusion study with CSF/$C_{u,p}$ values calculated using eq. 17

Infusion studies were performed for the RO1, RO2, RO3, RO4, and RO5 compounds. Measured CSF values indicated are mean values for three (RO1–4) or four (RO5) animals per group.

Compound	Bidirectional ER	Unidirectional AP-ER	Measured CSF/$C_{u,p}$ ±S.D.	Calculated CSF/$C_{u,p}$ using ER	Calculated CSF/$C_{u,p}$ using AP-ER
RO1	23	4	0.30 ± 0.10	0.05	0.25
RO2	5	1	0.59 ± 0.14	0.22	1.00
RO3	25	10	0.24 ± 0.03	0.04	0.10
RO4	22	10	0.12 ± 0.02	0.05	0.10
RO5	26	1.5	0.23 ± 0.02*	0.04	0.67

*Steady state not reached during 6-hour infusion.

and AP-ER. Depending on whether these "atypical" compounds are dosed from the A→B or B→A direction, their unusual physicochemical properties may contribute to an asymmetric interaction with P-gp and the cell membrane; in some extreme cases, $P_{app}^{A\rightarrow B}$ will be similar to the passive permeability whereas $P_{app}^{B\rightarrow A}$ will be more than 10 times higher (e.g., RO5 in Table 2). However, since P-gp is localized at the apical (blood-facing) membrane of polarized tissues, dosing in the B→A direction is not physiologically relevant to the BBB.

Alternatively, the difference between AP-ER and ER in this context may be due to a very large basolateral-cellular transport in the B→A direction leading to artificially high concentrations in the cells and, therefore, to greater P-gp–mediated transport than that observed in vivo.

AP-ER is a Superior Parameter to Estimate In Vivo CSF/$C_{u,p}$ Concentration Ratios in Rats. CSF concentrations are often assumed to be similar to brain extracellular fluid concentrations in vivo and considered the best surrogate for measuring free concentrations in brain (Westerhout et al., 2013). Considering the large difference between ER and AP-ER for ~40% of compounds from our in-house data base, the question arises as to which parameter more accurately predicts in vivo brain penetration. A number of publications describe good correlation between free plasma concentration normalized by the ER and measured CSF concentration in rodents and nonhuman primates (Ohe et al., 2003; Tang et al., 2009; Caruso et al., 2013). Using previously reported rat CSF and free plasma concentration values, we reestablished the reported correlations with ER and compared the results with those obtained using AP-ER. We show that using AP-ER instead of ER results in some improvement in statistical parameters of the linear regression model with the reported CSF concentrations in rats. Since this data set does not contain a compound with a large difference between ER and AP-ER, we selected compounds (RO1–5) that had an ER 2.2- to 17-fold larger than AP-ER for further investigation. Taking RO1 as an example, according to eq. 17, the expected concentration for this compound in rat CSF is about six times higher when using AP-ER versus ER. Experimental results reveal that measured steady state CSF concentration is identical with the estimated CSF exposure when using free plasma concentration and AP-ER. Conversely, calculated CSF exposure is about six times lower when using ER instead of AP-ER. The four other compounds tested also showed that AP-ER predicts measured CSF concentration more accurately than ER. In the presence of tariquidar, a selective P-gp inhibitor, we found that the measured CSF concentration is comparable to the free plasma concentration, confirming that P-gp is the only involved transporter contributing to efflux of these compounds (data not shown).

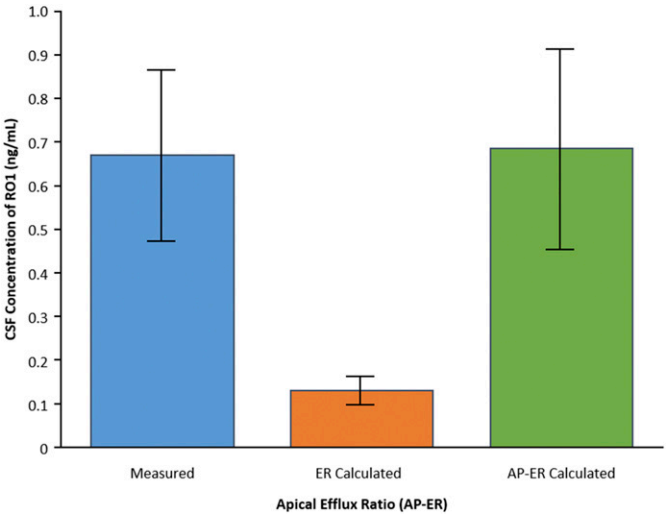

Fig. 3. Results of the in vivo rat study after bolus injection followed by an infusion of RO1 for 6 hours before CSF was taken. Values represent the mean concentration with S.D. from three animals. Blue bar: measured CSF concentration. Orange bar: calculated CSF concentration (eq. 17) using the free plasma concentration and the bidirectional efflux ratio (ER = 23). Green bar: calculated CSF concentration (eq. 17) using the free plasma concentration and the apical efflux ratio (AP-ER = 4). Calculated CSF concentration using the AP-ER is identical to the measured CSF concentration, showing that AP-ER provides a better measure to estimate the in vivo P-gp–mediated efflux properties of RO1 in rats.

Importantly, similar results were achieved in the human model (MDR1 protein; Supplemental Figure 1 and Fischer et al., 2020), where AP-ER was more accurate than ER in predicting CSF concentration of compounds. This suggests that AP-ER/ER ratios may be conserved for at least two species and that the mechanism underlying a larger difference between AP-ER and ER is mainly driven by the physicochemical properties of a compound.

Conclusions

The novel, more physiologically relevant, unidirectional AP-ER model has previously been suggested to predict P-gp–mediated transport of compounds more accurately than the classic bidirectional ER model across animal models (Fischer et al., 2020). In rat infusion studies, where CSF was taken at a time point at which steady state can be assumed, we have demonstrated that CSF estimations based on the AP-ER model are superior to those based on ER. Furthermore, we also confirmed this observation, over the past 7 years, in numerous single-dose pharmacokinetic experiments in rats and mice where CSF was taken 1–2 hours after compound administration (data

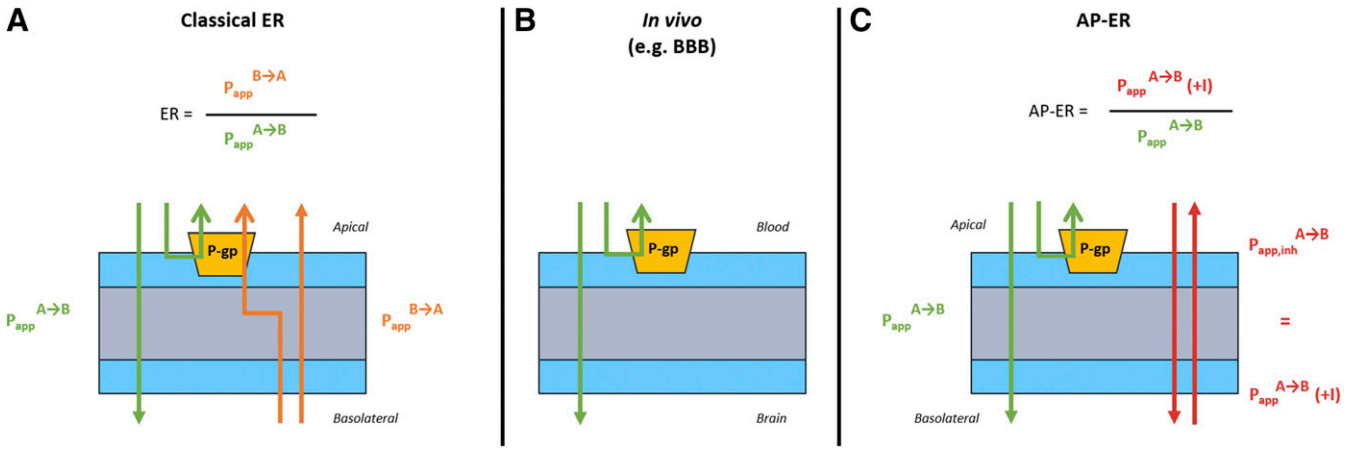

Fig. 4. Schematic depiction of the calculation of the classic bidirectional ER (A), P-gp–mediated transport through the blood-brain barrier (B), and the unidirectional AP-ER (C). (A) The classic, bidirectional ER model is calculated as a ratio of apparent permeability values in the B→A and A→B directions. (B) In vivo, P-gp is located at the apical side of the blood-brain barrier and transports compounds in the A→B direction only (unidirectional transport). (C) The novel AP-ER model is a ratio of permeability rates with and without a P-gp inhibitor at the apical site: in the presence of a P-gp inhibitor, the passive B→A and A→B permeability rates are considered equivalent, similar to in vivo conditions. P_{app} (+I), apparent permeability in the presence of an inhibitor. Fischer H., Ullah M., de la Cruz C.C., et al. Entrectinib, a TRK/ROS1 inhibitor with anti-CNS tumor activity: differentiation from other inhibitors in its class due to weak interaction with P-glycoprotein. Neuro-Oncology 2020; 22(6): 819–829 doi:10.1093/neuonc/noaa052. Reprinted by permission of Oxford University Press on behalf of the Society for Neuro-Oncology.

not shown). Although single-point CSF measurements after 1–4 hours will not guarantee that steady-state conditions are reached, they are a good first estimate of the anticipated brain exposure of compounds and are common practice in the early discovery phase. Importantly, we have recently reported that the superiority of AP-ER over ER is clinically relevant for entrectinib, a selective inhibitor of tropomyosin receptor kinase (TRK) A/B/C, C-ros oncogene 1 (ROS1), and anaplastic lymphoma kinase (ALK) (Fischer et al., 2020).

In this report, we investigated the reasons underlying the discrepancy between the ER and AP-ER models using a large range of compounds with different chemical properties. Furthermore, we attempted to group our chemical series according to P-gp substrates where this disparity could be rationalized based on the influence of passive permeability or the direct interaction with P-gp. Our results highlight that the ER model can overestimate the in vivo situation in rodents for up to ~40% of compounds and provide valuable insight into the physicochemical properties of compounds for which AP-ER is a much better predictor of brain penetration in vivo. This knowledge could allow P-gp in vitro screening processes to be adapted to use the less resource-intensive AP-ER model instead of the classic ER. It is also reasonable to speculate that AP-ER might be a better model than ER to address the influence of P-gp in limiting drug absorption in tissues other than the BBB, such as in the small intestine after oral administration. Although further work is needed to examine this, AP-ER has the potential to refine the definition of P-gp substrates at the intestine, which may have implications on current guidance from health authorities on drugs interacting with P-gp and the associated requirement for drug-drug interaction studies where substrates are identified (US Food and Drug Administration/Center for Drug Evaluation and Research, 2020).

Overall, we believe that these results may not only help to save in vivo and in vitro resources, contributing to the Replacement, Reduction, and Refinement initiative for animal experiments, but also increase our understanding and optimization of the properties and structural residues that contribute to high P-gp–mediated efflux of compounds in vivo.

Acknowledgments

We would like to thank Antonello Caruso and Michael Gertz for their advice on model development, as well as Urs Bader, Marie-Elise Brun, Veronique Dall'Asen, Anne-Christine Cascais, Pawel Dzygiel, Marie-Stella Gruyer, Catherine Karrer, Christelle Rapp, and Peter Schrag for their excellent experimental support on this work. Third-party medical writing assistance, under the direction of the authors, was provided by Laura Vergoz, of Gardiner-Caldwell Communications, and was funded by F. Hoffmann-La Roche Ltd.

Authorship Contributions

Participated in research design: Fischer, Senn, Ullah, Cantrill, Schuler, Yu.

Conducted experiments: Senn, Ullah, Cantrill.

Contributed new reagents or analytic tools: Fischer, Senn, Ullah, Cantrill, Schuler, Yu.

Performed data analysis: Fischer, Senn, Ullah, Cantrill, Schuler, Yu.

Wrote or contributed to the writing of the manuscript: Fischer, Senn, Ullah, Cantrill, Schuler, Yu.

References

Banker MJ, Clark TH, and Williams JA (2003) Development and validation of a 96-well equilibrium dialysis apparatus for measuring plasma protein binding. *J Pharm Sci* **92**:967–974.

Bankstahl JP, Kuntner C, Abrahim A, Karch R, Stanek J, Wanek T, Wadsak W, Kletter K, Müller M, Löscher W, et al. (2008) Tariquidar-induced P-glycoprotein inhibition at the rat blood-brain barrier studied with (R)-11C-verapamil and PET. *J Nucl Med* **49**:1328–1335.

Bednarczyk D and Sanghvi MV (2020) The impact of assay recovery on the apparent permeability, a function of lysosomal trapping. *Xenobiotica* **50**:753–760.

Brouwer KL, Keppler D, Hoffmaster KA, Bow DA, Cheng Y, Lai Y, Palm JE, Stieger B, and Evers R; International Transporter Consortium (2013) In vitro methods to support transporter evaluation in drug discovery and development. *Clin Pharmacol Ther* **94**:95–112.

Caruso A, Alvarez-Sánchez R, Hillebrecht A, Poirier A, Schuler F, Lavé T, Funk C, and Belli S (2013) PK/PD assessment in CNS drug discovery: prediction of CSF concentration in rodents for P-glycoprotein substrates and application to in vivo potency estimation. *Biochem Pharmacol* **85**:1684–1699.

De Lange ECM, Vd Berg DJ, Bellanti F, Voskuyl RA, and Syvänen S (2018) P-glycoprotein protein expression versus functionality at the blood-brain barrier using immunohistochemistry, microdialysis and mathematical modeling. *Eur J Pharm Sci* **124**:61–70.

Desai PV, Sawada GA, Watson IA, and Raub TJ (2013) Integration of in silico and in vitro tools for scaffold optimization during drug discovery: predicting P-glycoprotein efflux. *Mol Pharm* **10**:1249–1261.
Eytan GD, Regev R, Oren G, Hurwitz CD, and Assaraf YG (1997) Efficiency of P-glycoprotein-mediated exclusion of rhodamine dyes from multidrug-resistant cells is determined by their passive transmembrane movement rate. *Eur J Biochem* **248**:104–112.
Fischer H, Ullah M, de la Cruz CC, Hunsaker T, Senn C, Wirz T, Wagner B, Draganov D, Vazvaei F, Donzelli M, et al. (2020) Entrectinib, a TRK/ROS1 inhibitor with anti-CNS tumor activity: differentiation from other inhibitors in its class due to weak interaction with P-glycoprotein. *Neuro Oncol* **22**:819–829.
Giacomini KM, Galetin A, and Huang SM (2018) The international transporter consortium: summarizing advances in the role of transporters in drug development. *Clin Pharmacol Ther* **104**:766–771.
Hammarlund-Udenaes M, Fridén M, Syvänen S, and Gupta A (2008) On the rate and extent of drug delivery to the brain. *Pharm Res* **25**:1737–1750.
Higgins CF and Gottesman MM (1992) Is the multidrug transporter a flippase? *Trends Biochem Sci* **17**:18–21.
Kikuchi R, de Morais SM, and Kalvass JC (2013) In vitro P-glycoprotein efflux ratio can predict the in vivo brain penetration regardless of biopharmaceutics drug disposition classification system class. *Drug Metab Dispos* **41**:2012–2017.
Kuteykin-Teplyakov K, Luna-Tortós C, Ambroziak K, and Löscher W (2010) Differences in the expression of endogenous efflux transporters in MDR1-transfected versus wildtype cell lines affect P-glycoprotein mediated drug transport. *Br J Pharmacol* **160**:1453–1463.
Landwojtowicz E, Nervi P, and Seelig A (2002) Real-time monitoring of P-glycoprotein activation in living cells. *Biochemistry* **41**:8050–8057.
Litman T, Zeuthen T, Skovsgaard T, and Stein WD (1997) Structure-activity relationships of P-glycoprotein interacting drugs: kinetic characterization of their effects on ATPase activity. *Biochim Biophys Acta* **1361**:159–168.
Milletti F, Storchi L, Sforna G, and Cruciani G (2007) New and original pKa prediction method using grid molecular interaction fields. *J Chem Inf Model* **47**: 2172–2181.
Miyamoto R, Nozawa T, Shiozuka K, and Tabata K (2019) The impact of endogenous breast cancer resistance protein on human P-glycoprotein-mediated transport assays using LLC-PK1 cells transfected with human P-glycoprotein. *J Pharm Sci* **108**:1085–1089.
Ohe T, Sato M, Tanaka S, Fujino N, Hata M, Shibata Y, Kanatani A, Fukami T, Yamazaki M, Chiba M, et al. (2003) Effect of P-glycoprotein-mediated efflux on cerebrospinal fluid/plasma concentration ratio. *Drug Metab Dispos* **31**:1251–1254.
Ohashi R, Watanabe R, Esaki T, Taniguchi T, Torimoto-Katori N, Watanabe T, Ogasawara Y, Takahashi T, Tsukimoto M, and Mizuguchi K (2019) Development of simplified in vitro P-glycoprotein substrate assay and in silico prediction models to evaluate transport potential of P-glycoprotein. *Mol Pharm* **16**:1851–1863.
Pleban K, Kopp S, Csaszar E, Peer M, Hrebicek T, Rizzi A, Ecker GF, and Chiba P (2005) P-glycoprotein substrate binding domains are located at the transmembrane domain/transmembrane domain interfaces: a combined photoaffinity labeling-protein homology modeling approach. *Mol Pharmacol* **67**:365–374.
Poirier A, Cascais AC, Bader U, Portmann R, Brun ME, Walter I, Hillebrecht A, Ullah M, and Funk C (2014) Calibration of in vitro multidrug resistance protein 1 substrate and inhibition assays as a basis to support the prediction of clinically relevant interactions in vivo. *Drug Metab Dispos* **42**:1411–1422.
Pottier G, Marie S, Goutal S, Auvity S, Peyronneau MA, Stute S, Boisgard R, Dollé F, Buvat I, Caillé F, et al. (2016) Imaging the impact of the P-glycoprotein (ABCB1) function on the brain kinetics of metoclopramide. *J Nucl Med* **57**:309–314.
Saaby L and Brodin B (2017) A critical view on in vitro analysis of p-glycoprotein (P-gp) transport kinetics. *J Pharm Sci* **106**:2257–2264.
Schinkel AH, Mol CAAM, Wagenaar E, van Deemter L, Smit JJM, and Borst P (1995) Multidrug resistance and the role of P-glycoprotein knockout mice. *Eur J Cancer* **31A**:1295–1298.
Schwab D, Fischer H, Tabatabaei A, Poli S, and Huwyler J (2003) Comparison of in vitro P-glycoprotein screening assays: recommendations for their use in drug discovery. *J Med Chem* **46**:1716–1725.
Schou M, Varnäs K, Lundquist S, Nakao R, Amini N, Takano A, Finnema SJ, Halldin C, and Farde L (2015) Large variation in brain exposure of reference CNS drugs: a PET study in nonhuman primates. *Int J Neuropsychopharmacol* **18**:pyv036.
Shapiro AB and Ling V (1997) Extraction of Hoechst 33342 from the cytoplasmic leaflet of the plasma membrane by P-glycoprotein. *Eur J Biochem* **250**:122–129.
Tang C, Kuo Y, Pudvah NT, Ellis JD, Michener MS, Egbertson M, Graham SL, Cook JJ, Hochman JH, and Prueksaritanont T (2009) Effect of P-glycoprotein-mediated efflux on cerebrospinal fluid concentrations in rhesus monkeys. *Biochem Pharmacol* **78**:642–647.
Tournier N, Bauer M, Pichler V, Nics L, Klebermass EM, Bamminger K, Matzneller P, Weber M, Karch R, Caillé F, et al. (2019) Impact of P-glycoprotein function on the brain kinetics of the weak substrate 11C-Metoclopramide assessed with PET imaging in humans. *J Nucl Med* **60**:985–991.
Thiel-Demby VE, Tippin TK, Humphreys JE, Serabjit-Singh CJ, and Polli JW (2004) In vitro absorption and secretory quotients: practical criteria derived from a study of 331 compounds to assess for the impact of P-glycoprotein-mediated efflux on drug candidates. *J Pharm Sci* **93**:2567–2572.
US Food and Drug Administration/Center for Drug Evaluation and Research (2020) In Vitro Drug Interaction Studies — Cytochrome P450 Enzyme- and Transporter-Mediated Drug Interactions. Guidance for Industry. Center for Drug Evaluation and Research, US Food and Drug Administration, Silver Spring, MD.
Westerhout J, Smeets J, Danhof M, and de Lange EC (2013) The impact of P-gp functionality on non-steady state relationships between CSF and brain extracellular fluid. *J Pharmacokinet Pharmacodyn* **40**:327–342.
Wise JG (2012) Catalytic transitions in the human MDR1 P-glycoprotein drug binding sites. *Biochemistry* **51**:5125–5141.
Zamek-Gliszczynski MJ, Ruterbories KJ, Ajamie RT, Wickremsinhe ER, Pothuri L, Rao MVS, Basavanakatti VN, Pinjari J, Ramanathan VK, and Chaudhary AK (2011) Validation of 96-well equilibrium dialysis with non-radiolabeled drug for definitive measurement of protein binding and application to clinical development of highly-bound drugs. *J Pharm Sci* **100**:2498–2507.

Address correspondence to: Holger Fischer, F. Hoffmann-La Roche Ltd., Bldg. 001/07.NBH04, CH-4070 Basel, Switzerland. E-mail: Holger.fischer@roche.com